Photonic valence/conduction subbands in optically generated photonic quantum wells: Tunable optical-delay line application

S. M. Sadeghi*
Department of Physics, University of Alabama in Huntsville, Huntsville, Alabama 35899, USA

W. Li
Department of Chemistry and Engineering Physics, University of Wisconsin–Platteville, Platteville, Wisconsin 53818, USA

(Received 18 March 2009; revised manuscript received 17 June 2009; published 21 July 2009)

It has been shown that, in the absence of a control laser field, functional photonic superstructures can act as homogeneous photonic band gap structures formed via uniform corrugations of their background refractive indexes. When some sections of these structures are illuminated with such a laser, those sections become resonant (active) photonic band structures with higher refractive index contrast, forming photonic heterostructures. In this paper we study how by controlling the phase of quantum interference processes in such structures one can control alignment of such heterostructures, coherently generating photonic quantum wells with either conduction- or valencelike subbands (resonant transmission states). We show the energies of these subbands can be tuned by the control laser and demonstrate that their longitudinal mode profiles follow one-by-one correspondence with the envelope functions of the electron or hole subbands in electronic quantum well structures. In particular, we show how such photonic quantum wells can act as optically tunable time-delay lines, capable of increasing delay of a signal passing through them significantly via laser-induced control of optical confinements of the photonic subbands.

DOI: 10.1103/PhysRevB.80.045316 PACS number(s): 42.70.Qs, 78.67.De, 42.50.−p

I. INTRODUCTION

Photonic structures can confine photons similar to the ways semiconductor (electronic) quantum wells (QWs), wires or dots confine electrons. This is an appealing subject of research as it can have numerous applications, both from practical and fundamental point of views. These applications are ranging from super small laser cavities to quantum electrodynamics of quantum dots.[1,2] Construction of a photonic quantum dot has already been reported via patterning a planar optical microcavity structure.[3] Decrease of the lateral size of such structures can shift the optical modes of these structures to higher energies, analogous to what one expects in semiconductor quantum dots.[4] It has also been shown that by bringing two of such photonic quantum dots together one can also form a "photonic molecule."[5] In such a structure reduction of the length of the channel connecting the two dots can in fact increase energy splitting of the confined photonic modes. This is in close analogy to the emergence of electronic bonding and antibonding modes in diatomic molecules. Photonic quantum wells have also been studied by sandwiching a medium between photonic barriers. The presence of quantized confined states in such structures due to the photonic confinement effect, similar to that in the semiconductor quantum wells, has been investigated.[6,7]

Photon confinements in the cases mentioned above were generated by spatial variation of semiconductor materials, either by etching or forming heterostructures of semiconductor materials. In a recent paper we proposed a special type of photonic structures, called photonic superstructures (Fig. 1), that allow photonic barriers and confinement happen via coherent processes caused by a laser beam (control field).[8] These structures are in fact functional semiconductor waveguides that in the absence of the control field act as passive photonic band gap structures characterized by their background refractive index corrugations. When the control field illuminates one or several parts of such waveguides, those parts are transformed into active photonic band gap structures with much higher refractive index contrast. In other words, as shown in Figs. 1 and 2, the structure coherently becomes a monolithic tandem of passive and active PBG structures. Obviously the active PBG structures can be created at any location of the waveguide or can be moved from one location to another.

One of our objectives in this paper is to study how one can coherently control band alignment of passive and active photonic band gaps in photonic superstructures. In other words, we will study the unprecedented capability of such structures to form different types of optically generated photonic QWs. In semiconductor (electronic) structures alignment of electronic band gaps is an important issue, as it relates to whether a QW structure is type I or II, and determines its conduction and valence band offsets, transport properties, etc. In contrast to electronic heterostructures where band alignment is a rather predetermined structural

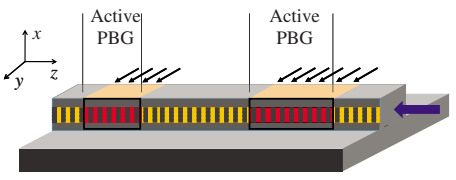

FIG. 1. (Color online) Overall concept of a photonic superstructure. Here the structure is a ridge waveguide that can be illuminated from the side by the control laser (horizontal arrows). The illuminated regions become active PBG with enhanced band gaps while the unilluminated region remains passive PBG with smaller band gap. The thick arrow along z refers to the signal beam.

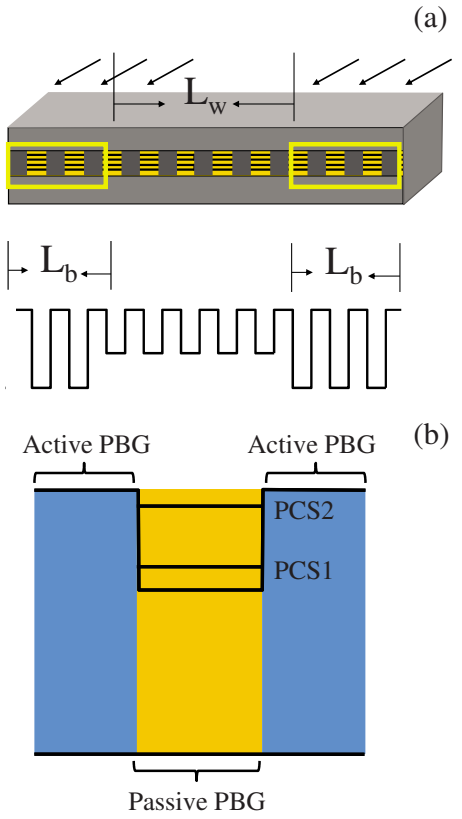

FIG. 2. (Color online) Schematic illustration of the coherently generated photonic QW with conductionlike band. In (a) the arrows refer to the control field beam illuminating the functional superstructure from the side in two locations. L_b refers to the length of the illuminated region (barrier), and L_w represents the width of the unilluminated region (well). (b) shows the band alignment of the passive and active PBGs when the infrared laser suppresses low refractive index regions [stepped line in (a)].

feature, in functional photonic superstructures we can adjust the control laser to set up specific forms of photonic band gap alignment. In one limit this can lead to formation of photonic QW structures with valencelike band.[8] In this case the photonic well is formed similar to a type I semiconductor QW with zero conduction band offset. As discussed in this paper, the other limit includes generation of photonic QW structures with conductionlike bands. The counterpart of this case in electronic structures includes type I QW structures wherein their valence offsets are zero (Fig. 2). Such photonic QWs support resonant transmission states or photonic subbands very similar to those in the conduction or valence band of semiconductor QWs. As shown in this paper, for example, the longitudinal mode profiles of the photonic conduction subbands (PCBs) introduced in this paper (Fig. 2) resemble consistently with the envelope functions of the conduction subbands in electronic QW structures.

Another objective of this paper is to show how photonic subbands (or resonant transmission states) studied in this paper allow us to use photonic superstructures as efficient tunable optical time-delay lines or optical buffers. Such applications are related to one of the main challenges existing today in optical communication, i.e., the ability to store an optical signal in optical format and being able to keep the data in optical domain during the routing process. Tunable optical-delay lines have recently been discussed extensively using slow light. In these cases one uses variation of group velocity of light mostly by application of another light.[9,10] In this paper we show that optical-delay lines based on photonic subbands discussed in this paper allow one to increase delay of a signal passing through a photonic superstructure significantly, going from picosecond delay range in the absence of the control field to nanosecond range when the photonic quantum well is formed. The results also show that one can spectrally tune the delayed signal. Such a significant delay is reached based on the fact that in the optically induced photonic QW presented in this paper, the width of the QW can be continuously controlled by changing the lengths of the two illuminated regions (photonic barriers). As a result, we not only can adjust the number of the photonic subbands and their energies, but also their linewidths.

II. COHERENTLY GENERATED PHOTONIC HETEROSTRUCTURES: REVIEW OF THE THEORY

The main idea in this paper is based on application of a laser field to spatially change the contrast of refractive index in designated regions of a functional waveguide. The ridge of such a waveguide (Fig. 1) contains a periodic corrugation of several periods of a semiconductor QW (SQW) structure along the z axis [Fig. 2(a)]. Because such a structural corrugation is considered uniform, in the absence of the control field it leads to a uniform refractive index perturbation and coupling coefficient. In other words, the whole waveguide structure contributes to the formation of a single PBG. When the control field influences a portion of this waveguide, however, the refractive index perturbation in that region increases. This changes the light scattering along the waveguide, setting up a photonic barrier or heterostructure.[8] As shown in Fig. 2 the increase of index perturbation here happens via coherent reduction of lower refractive index regions (SQW regions). As we will show in following this could lead to a specific photonic band gap alignment, generating a photonic QW structure as depicted in Fig. 2(b). Using a similar waveguide structure, or photonic superstructure, one can generate a different type of photonic band gap alignment, forming valencelike conduction bands. For this one needs to adjust the duty cycle of the corrugated SQW regions and use coherent effects to enhance their refractive indexes.[8] Note such enhancement and suppression of refractive index processes happen in the presence of electromagnetically induced transparency (EIT). Therefore, these processes occur without adding any loss to the photonic waveguide structures.

The SQW structure considered in this paper is an n-doped double structure as that shown in the inset of Fig. 3. The control laser field is near resonance with the 1–3 transition of this structure. In the presence of this field and the probe field near resonant with the 2–3 transition, quantum interference happens, increasing or decreasing the refractive index of this transition while allowing it to remain transparent at a given frequency range via formation of EIT. To study these issues we consider the double SQW structure contains a populated ground subband ($|1\rangle$) and two upper subbands ($|2\rangle$ and $|3\rangle$)

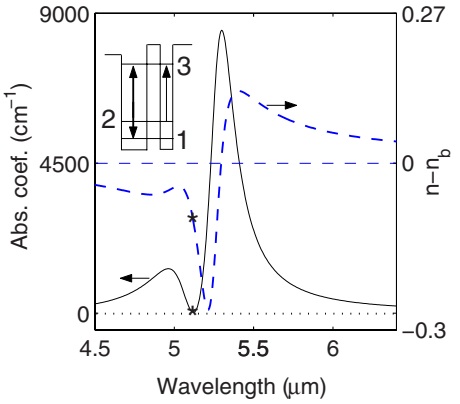

FIG. 3. (Color online) Absorption coefficient (solid line) and refractive index change (thick dashed line) of the 2–3 transition when I_c=0.7 MW/cm^2 and Δ_c=−4.1 meV. The stars indicate the wavelength where EIT happens. The horizontal dotted and dashed lines refer, respectively, to absorption and refractive index of this transition when I_c=0. The inset schematically shows the double semiconductor QW, wherein the double sided arrow refers to the coupling field and the one-sided one to the probe field.

(Fig. 3 inset). This structure contains 4 and 2 nm $In_{0.5}Ga_{0.5}As$ wells separated by 1.5 nm $Al_{0.5}Ga_{0.5}As$ barrier. The left and right barriers are, respectively, $Al_{0.4}Ga_{0.6}As$ and $Al_{0.55}Ga_{0.45}As$. Including the effects of strain and energy-dependent electron effective mass, we find a relatively large dipole moment for the 2–3 transition (μ_{23}=2.7$e\times$nm) with a transition wavelength of about 5.2 μm.[11] The 1–3 transition occurs at 3.17 μm with μ_{13}=0.8$e\times$nm. We considered the electron-electron scattering rate in the ground subband (Γ^{e-e}) was 4 ps^{-1} and the energy relaxation times of electrons from the third subband to the second and first subbands ($1/\Gamma_i$) were, respectively, 2 and 3 ps.[12,13] In addition, considering the 1–2 transition energy (152 meV) and the carrier density (7×10^{11} cm^{-2}), we assumed the tunneling time ($1/\Gamma_t$) from $|2\rangle$ to $|1\rangle$ was roughly 2.5 ps. The response of such a QW system at the vicinity of the 2–3 transition was obtained by solving the optical Bloch equations. In these equations the polarization dephasing rates (γ_{ij}) associated with the intersubband transitions were $\gamma_{13}=(\Gamma_3+\Gamma_2+\Gamma^{e-e})/2=2.41$, $\gamma_{12}=(\Gamma_t+\Gamma^{e-e})/2=2.2$, $\gamma_{23}=(\Gamma_2+\Gamma_3+\Gamma_t)/2=0.64$ ps^{-1}. This suggests that the coherent processes discussed in this paper can happen in sub-ps scales.

When the control field is off the 2–3 transition is basically transparent (Fig. 3, dotted line) with a refractive index equal to that of the background index of the QW structure (n_b) (horizontal dashed line). In the presence of this field the absorption coefficient (solid line) and refractive index (thick dashed line) of this transition can change dramatically. In particular if we consider the intensity of this field (I_c) is set to 0.7 MW/cm^2 and its detuning from the 1–3 transition (Δ_c) is −4.1 meV, as shown in Fig. 3, absorption of this system develops EIT around 5.1 μm (star). At the same wavelength the refractive index of the 2–3 transition is suppressed significantly.

To numerically treat coherent formation of photonic QW, note that the slowly varying part of the light wave in the structures considered here can be expressed as

$$E^{I_c}_{\omega_c}(\omega,z)=F^{I_c}_{\omega_c}(\omega,z)e^{-j\beta_0 z}+R^{I_c}_{\omega_c}(\omega,z)e^{j\beta_0 z}. \quad (1)$$

Here the indices emphasize on the fact the optical field propagation along the functional waveguide structure considered in this paper is strongly influenced by the intensity (I_c) and frequency (ω_c) of the control field. For the first order corrugation with period Λ considered here we have $\beta_0=\pi/\Lambda$. $F^{I_c}_{\omega_c}(\omega,z)$ and $R^{I_c}_{\omega_c}(\omega,z)$ refer to the forward and backward waves with frequency ω along z. To find these functions we adopt a transfer matrix method including the effects of the control field. The details of calculations are presented in Ref. 8. Briefly, using this method we have

$$\begin{bmatrix} F^{I_c}_{\omega_c}(\omega,L_t) \\ R^{I_c}_{\omega_c}(\omega,L_t) \end{bmatrix} = T^{I_c}_{\omega_c}(\omega,L_t)\begin{bmatrix} F^{I_c}_{\omega_c}(\omega,0) \\ R^{I_c}_{\omega_c}(\omega,0) \end{bmatrix}. \quad (2)$$

Here $T^{I_c}_{\omega_c}(\omega,L)$ refers to the total transfer matrix. For coherently induced photonic QWs considered in this paper this is given by

$$T^{I_c}_{\omega_c}(\omega,L)=T^{I_c}_{\omega_c}(\omega,L_b)T_p(\omega,L_w)T^{I_c}_{\omega_c}(\omega,L_b). \quad (3)$$

Here $T^{I_c}_{\omega_c}(\omega,L_b)$ refer the transfer matrices of the exposed regions forming the barriers. The unilluminated region forms the well is described by $T_p(\omega,L_W)$. Here L_W refers to the length of the unilluminated region. $L_t=2L_b+L_W$ is the total length of the waveguide. The elements of the transfer matrix were calculated using a set of frequency-dependent coupled mode equations describing propagation of light wave in a medium with perturbation of complex susceptibilities.[8,14,15] The susceptibility in turn was obtained by solving optical Bloch equations under steady state condition. Having real and imaginary parts of the susceptibility we calculated $\kappa^{I_c}_{\omega_c}(\omega)$, i.e., the field-dependent complex coupling coefficient of the structure. Obviously this parameter is different in different part of the structures, depending on whether it is influenced by the control field or not. Note that in this paper we used optical Bloch equations within relaxation time approximation. In general, however, when relaxation processes involve with significant changes in the transition energies,[16] or when the applied field is so strong that these processes become field dependent,[17] these equations may not be valid.

III. CONDUCTIONLIKE PHOTONIC BANDS

To study coherent generation of photonic QWs with conductionlike bands, we consider the waveguide structure contains 80 periods of the double SQW structure etched periodically with 813 nm period. The trenches are then refilled epitaxially with $In_xAl_{1-x}As$. The In content (x) is adjusted such that the effective refractive indices of these regions (trenches) are more than those of the QW regions in the absence of the control field. The substrate is GaAs and the lower confinement layer is a graded $In_xAl_{1-x}As$ layer, allowing accommodation of high strain and providing the optical confinement needed for the waveguide structure. The upper confinement layer is also taken to be $In_xAl_{1-x}As$ with an average refractive index of 3 in the vicinity of 5 μm, similar to that of the lower confinement layer.[18] We consider the

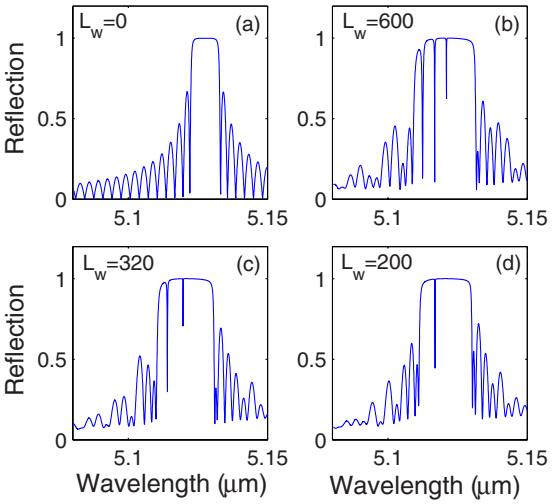

FIG. 4. (Color online) Reflection of the waveguide structure when two regions of the waveguide are illuminated by the control field [Fig. 2(a)]. The intensity and wavelength of the laser are considered to be similar to those in Fig. 3. The numbers on the left top corners refer to the width of the unilluminated region (L_w in μm).

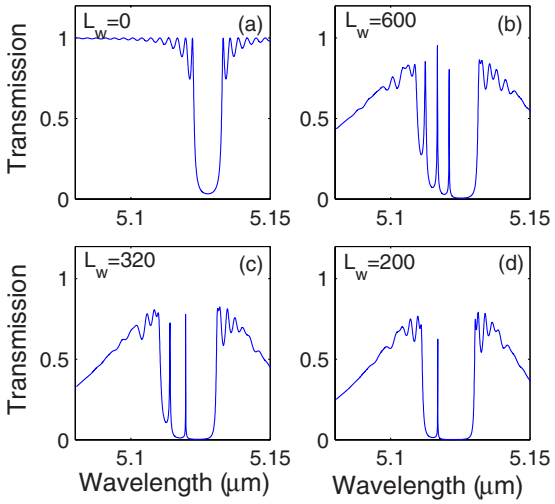

FIG. 5. (Color online) Corresponding transmission of waveguide structure studied in Fig. 4. All parameters are the same as those in Fig. 4.

facets are AR coated and the double SQWs are located a narrow-width ridge illuminated from the side by the control field (Fig. 1). This allows us to ignore variation of the control field intensity.

In this section the widths of the barriers formed by the coherent effects are considered to be the same. We vary the magnitudes of these barriers (L_b) by controlling the widths of the illuminated regions. The intensity of the control field is considered 0.7 MW/cm^2 and we assume it is detuned from the 1–3 transition by −4.1 meV. The results of calculations are rather unique. For L_t=1200 μm, as shown in Fig. 4(a), when L_b=0 (or I_c=0), we have a well-developed PBG. When the width of each barrier L_b=300 μm (L_w=600 μm) we see significant changes in the band gap. These include enhancement of the band gap from the shorter wavelength side and formation of some very sharp resonances within that region [Fig. 4(b)]. The larger L_b becomes, i.e., the smaller L_w is, the number of these ultrasharp transmission resonances are reduced while they undergo blue energy shifting. For L_b =440 μm or L_w=320 μm [Fig. 4(c)], there exist basically two transmission resonances in the band gap. For L_b =500 μm or L_w=200 μm [Fig. 4(d)], the number of resonances is reduced to one.

Figure 5 shows the corresponding transmission of the system. Note for L_w=0, we have a homogeneous passive PBG. Therefore, as shown in Fig. 5(a), except around the band gap where Bragg scattering happens, transmission is frequency independent. When the infrared laser illuminates the waveguide, the illuminated parts form resonant PBG structures. Such structures are only lossless around the main frequency where EIT happens. Therefore, the reduction of transmission around the band gap in Figs. 5(b)–5(d) is due to the absorption of the 2–3 transitions away from the minimum absorption of EIT (Fig. 3, star).

The results presented in Figs. 4 and 5 are analogous to the conduction subbands of single electronic QW structures. In such structures the number of the subbands depends on the width and the band offset of the QW. The transmission resonances seen in Figs. 4 and 5 are formed inside the shorter wavelength transparent region of the passive region. As one can see, under no condition any state is formed inside the longer wavelength region of the band gap. The number and energies of such photonic conduction subbands (Fig. 4) also seem to follow the same rules as the conduction subbands of semiconductor QWs. The blue shift of the photonic resonances (subbands) toward shorter wavelengths is particularly consistent with this argument. Note that using similar waveguide structure but with slightly different duty cycle for the corrugated SQW, one can generate valencelike photonic band. This happens when the control laser field causes enhancement of refractive index accompanied by EIT.[8] In such a case the photonic subbands happen at the longer wavelength side of the passive PBG and with the decrease of L_w they are pushed toward lower energies.

The longitudinal profile at each transmission resonance in Figs. 4 or 5 provides a consistent picture of formation of laser-induced photonic subbands. To see this in Fig. 6 (solid lines) we plot the squared values of combined forward and background waves ($|F^{I_c}_{\omega_c}+R^{I_c}_{\omega_c}|^2$) or longitudinal mode profile associated with each photonic conduction subband for the case of L_w=600 μm (L_b=300 μm). For such a photonic QW the three bound conduction subbands (PCB1, PCB2, and PCB3) are located at 5121.0 (a), 5116.75 (b), and 5112.4 nm (c), respectively. Figure 6(a) (PCB1) shows significant confinement with near zero leakage of light outside of the structure. The second and third subbands, however, are less confined, as one expects. These results are very similar to the envelope functions of electrons in electronic QW structures. This becomes more obvious if we consider the real (dashed lines) and imaginary (dotted lines) of $F^{I_c}_{\omega_c}+R^{I_c}_{\omega_c}$ for each photonic conduction subband. Note that, although $F^{I_c}_{\omega_c}+R^{I_c}_{\omega_c}$ is complex, both its real and imaginary parts show significant similarities with the wave functions of conduction subbands in single SQW, even in terms of their parties.

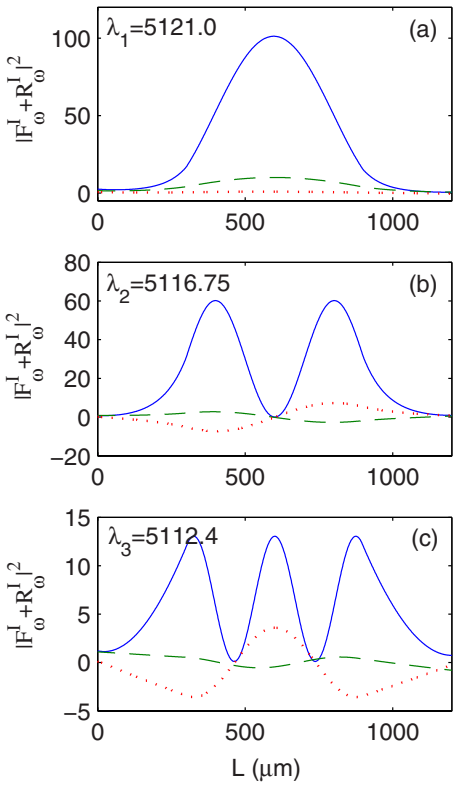

FIG. 6. (Color online) Longitudinal mode profiles ($|F^I_\omega+R^I_\omega|^2$) associated with the three transmission resonance peaks in Fig. 4(b) (solid lines). The dashed and dotted lines refer, respectively, to the real and imaginary parts of $F^I_\omega+R^I_\omega$. λ_i (in nm) refers the wavelength of the ith photonic subband.

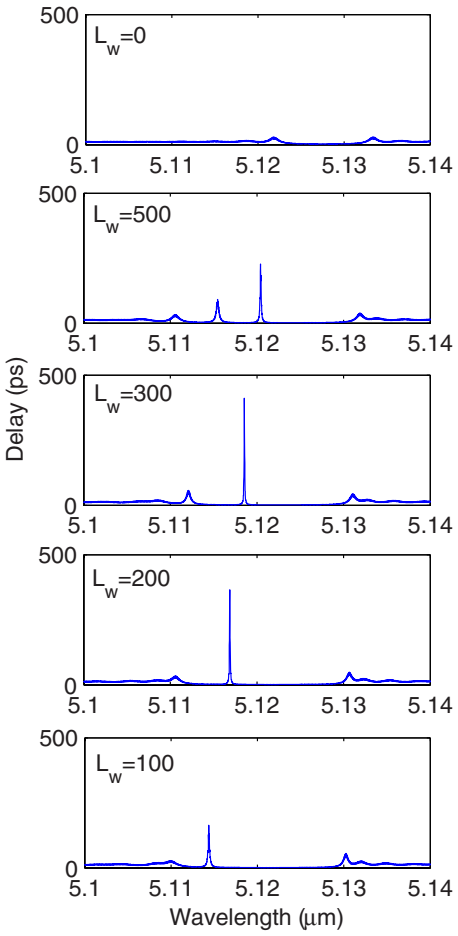

FIG. 7. (Color online) Time delays associated with the coherently generated photonic subbands in Fig. 5.

IV. TUNABLE OPTICAL DELAY LINE BASED ON PHOTONIC SUBBANDS

The results presented in Fig. 4 not only predict formation of photonic QW with optically tunable conduction subbands, but also reveal some other unique features. These include optical control of the photonic confinements of these subbands. Combination of these features allows one to envision various device applications. As an example in this section we study application of photonic superstructures as tunable optical-delay lines. As mentioned in the introduction, tunable optical-delay lines are of significant interest in optical communications. Optical time delays have been conventionally generated by varying a free-space or optical waveguide propagation path, choosing from a combination of predesigned optical path lengths.[19] Recently, however, delay based on slow light has also captured much attention for achieving continuously tunable optical delays.[9,10] In principle, slow light is achieved by tailoring an enhanced group index resonance within a given nonlinear medium. The delay line presented in this paper is based continuous control of photonic confinement and provides significant delay by just adjusting the control field illuminating the superstructure.

To start in Fig. 7 we present the results of calculations for the time delay of light passing through similar waveguide structure as that considered in Fig. 4. Here, however, we consider $L_t=1000$ μm to avoid numerical implications caused by the very narrow transmission lines when L_w is small. As one can see here when $L_b=0$ (or $I_c=0$) for wavelengths around 5.12 μm and shorter the time delay is very small (about 10 ps). In the presence of control field ($I_c=0.7$ MW/cm^2) and for various values of L_b (or L_w) the results in Fig. 7 show that formation of photonic conduction subbands come with significant increase of time delay. In fact tracking the first subband (PCB1) suggests that for $L_w=300$ μm the time delay can reach over 400 ps. The overall results also show continuous tuning of the wavelength of the delayed signal. This also suggests ultranarrow wavelength selectivity for functional optical filters, ultrafast switches, and midinfrared spectroscopy.

Figure 7 shows that as L_w increases the amount of delay reaches a maximum and then starts to decrease. This issue can be related to the optical confinement of the mode causing the delay (PCB1). To see this in Fig. 8 we show the corresponding longitudinal profiles of this mode for three values of L_w considered in Fig. 7. As seen here, PCB1 has the maximum optical confinement when L_w is around 300 μm. For much larger L_w the barrier width is small and for smaller L_w the photonic subband is very close to the edge. Therefore, in both of these cases we see less optical confinement and time delay.

To see the impact of total length of the waveguide (L_t) in Fig. 9(a) we show variation of the time delay of the photonic

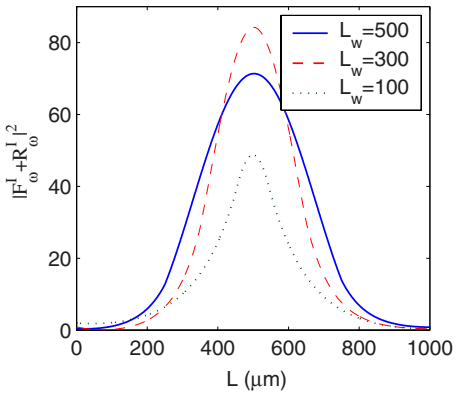

FIG. 8. (Color online) Variation of longitudinal mode profiles associated with Fig. 7 for three different values of L_w in μm (numbers in legends).

QW for $L_w=200$ μm and narrower when $L_t=800$ μm. Here one can see that the amount of delay is dropped drastically, compare to Fig. 7. Additionally, this figure shows how PCB1 can dominantly determine the overall time delay of the waveguide. The results also show that as the delayed signal is continuously detuned toward shorter wavelengths with reduction of L_w, the width of the transmitted spectrum increases. In other words, the photonic subband becomes broader. As shown in Fig. 9(b), such a broadening can be consistently related to the fact that with the decrease of L_w the mode associated with this subband becomes less localized.

Note also that the results presented in Fig. 3, and therefore in Fig. 4, are the results of quantum interference caused by the both probe and control fields. In fact these interference processes are very similar to those in systems exhibiting EIT.[20] Here, however, the interfering 1–3 (indirect) and 2–3 (direct) paths deal with significant electron population in the states mixed by the control field. One major feature, however, here is that the change of the control field detuning sign acts as a change of a phase in the interference process. As shown in Fig. 3, this leads to suppression of refractive index of the 2–3 transition.

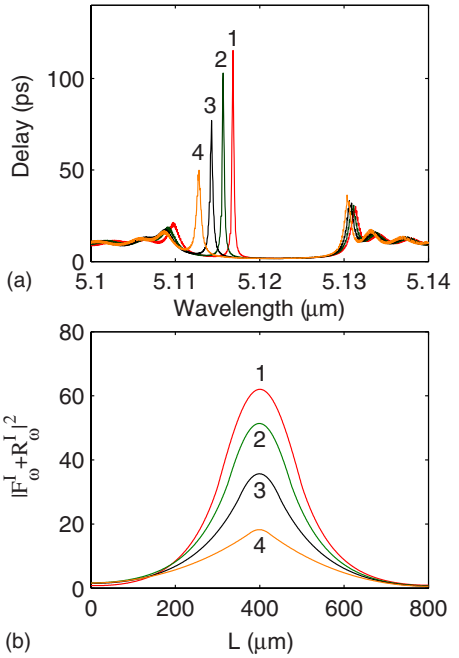

FIG. 9. (Color online) Time delay of the photonic superstructure considered in Fig. 7 but for $L_t=800$ μm (a). Peaks indicated with 1, 2, 3, and 4 refer, respectively, to $L_w=200$, 150, 100, and 50 μm. (b) shows their corresponding longitudinal mode profiles.

V. CONCLUSIONS

We studied coherent formation of photonic quantum wells using an infrared laser field. This laser was responsible for coherent formation of active photonic band gaps with relatively wide band gaps, acting as electromagnetically induced photonic barriers. The well was a passive PBG with smaller band gap. The barriers were the parts of a functional waveguide structure that were illuminated with a laser field, while the unilluminated part acted as the well. We showed that the photonic subbands were either conduction- or valencelike, i.e., with narrowing the well their subband energies blue- or redshifted, respectively. The widths of the photonic quantum wells discussed in this paper can be dynamically varied by just changing the lengths of the illuminated regions of the waveguide. This allows us to tune photonic subbands and changing their widths or numbers.

*seyed.sadeghi@uah.edu

[1] H. Altug, D. Englund, and J. Vuckovic, Nat. Phys. **2**, 484 (2006).
[2] A. Kiraz, C. Reese, B. Gayral, L. D. Zhang, W. V. Schoenfeld, B. D. Gerardot, P. M. Petroff, E. L. Hu, and A. Imamoglu, J. Opt. B: Quantum Semiclassical Opt. **5**, 129 (2003).
[3] J. P. Reithmaier, M. Rohner, H. Zull, F. Schafer, A. Forchel, P. A. Knipp, and T. L. Reinecke, Phys. Rev. Lett. **78**, 378 (1997).
[4] G. Schedelbeck, W. Wegscheider, M. Bichler, and G. Abstreiter, Science **278**, 1792 (1997).
[5] M. Bayer, T. Gutbrod, J. P. Reithmaier, A. Forchel, T. L. Reinecke, P. A. Knipp, A. A. Dremin, and V. D. Kulakovskii, Phys. Rev. Lett. **81**, 2582 (1998).
[6] J. Zi, J. Wan, and C. Zhang, Appl. Phys. Lett. **73**, 2084 (1998).
[7] Y. Jiang, C. Niu, and D. L. Lin, Phys. Rev. B **59**, 9981 (1999).
[8] S. M. Sadeghi, W. Li, X. Li, and W.-P. Huang, Phys. Rev. B **77**, 125313 (2008).
[9] R. W. Boyd and D. J. Gauthier, Prog. Opt. **43**, 497 (2002).
[10] C. J. Chang-Hasnain and S. L. Chuang, J. Lightwave Technol. **24**, 4642 (2006).
[11] T. Asano, S. Noda, T. Abe, and A. Sasaki, J. Appl. Phys. **82**, 3385 (1997).
[12] J. Faist, F. Capasso, C. Sirtori, D. L. Sivco, J. Baillargeon, A. L. Hutchinson, S.-N. G. Chu, and A. Y. Cho, Appl. Phys. Lett. **68**,

3680 (1996).
[13] O. Gauthier-Lafaye, S. Sauvage, P. Boucaud, F. H. Julien, F. Glotin, R. Prazeres, J.-M. Ortega, and V. T.-M. M. Planel, J. Appl. Phys. **83**, 2920 (1998).
[14] S. M. Sadeghi, X. Li, W.-P. Huang, and W. Li, J. Appl. Phys. **101**, 123107 (2007).
[15] S. M. Sadeghi, W. Li, X. Li, and W.-P. Huang, IEEE J. Quantum Electron. **42**, 752 (2006).
[16] P. R. Berman, J. Opt. Soc. Am. B **3**, 564 (1986).
[17] S. Singh and G. S. Agarwal, J. Opt. Soc. Am. B **5**, 254 (1988).
[18] D. S. Katzer, W. S. Rabinovich, and G. Beadie, J. Vac. Sci. Technol. B **18**, 1614 (2000).
[19] S. A. Hamilton, B. S. Robinson, T. E. Murphy, S. J. Savage, and E. P. Ippen, J. Lightwave Technol. **20**, 2086 (2002).
[20] K.-J. Boller, A. Imamoglu, and S. E. Harris, Phys. Rev. Lett. **66**, 2593 (1991).